

Efficient Ego Lane Detection for Various Lane Types

Rebekka Charlotte Peter*, Yuduo Song*, and Martin Lauer

Karlsruhe Institute of Technology
Institute for Measurement and Control Systems
Engler-Bunte-Ring 21, 76131 Karlsruhe

Abstract In this work, we present an ego lane detector designed for the use in automotive vision systems for personal light electric vehicles like electric bicycles, tricycles or scooters. The approach is based on a combination of gradient-based line detection, color-based segmentation and geometrical rules, making the ego lane detector fast, but also robust to different scenes, including curves. Qualitative evaluation on over fifty traffic scenes show that the lane detector is able to find a suitable approximation of the road area with an IoU of 75.71%.

Keywords Ego lane detection, color-based segmentation, vanishing point detection

1 Introduction

In recent years, personal light electric vehicles like electric scooters, bicycles or tricycles have been gaining in popularity. Being small and lightweight, they represent an emission free alternative to cars or a *last-mile* extension to public transportation systems. To increase safety and comfort of users, automation and driving assistance systems as for autonomous vehicles are conceivable. Even though the use-case appears to be similar, certain differences between personal light electric vehicles and cars make the direct application of algorithms difficult: As the product costs for personal light electric vehicles are significantly lower in comparison to cars, the reasonable

* These authors contributed equally.

maximum costs for sensors as well as computation hardware is lower in the same way. The same applies for a lower possible power consumption of the sensors and computation hardware, as the overall system offers less power. Existing algorithms for autonomous cars must be adapted to new traffic scenes and areas, as personal light electric vehicles are not restricted to drive on streets, but they can also use bicycle lanes or pedestrian paths. Aforementioned differences make especially the application of deep learning methods not readily transferable, firstly, because of the restricted hardware options, secondly, because of the variation in the input data to the training data sets for that the autonomous driving algorithms are optimized for. Moreover, learning-based methods can not merely be retrained because of the lack of datasets including traffic scenes of pedestrian paths and bicycle lanes or related traffic signs etc.

This work presents an algorithm for detecting the two borders of the lane, on which the ego vehicle, more precisely the ego bicycle, is. The above mentioned requirements for low-cost sensors and computation hardware as well as the applicability in various kinds of traffic scenes are fulfilled. Possible applications using ego lane detection include, for instance, obstacle detection on the ego lane or the usage of the ego lane information for traffic scene classification. The lane border detection system works on RGB images taken from a camera mounted on the handle bar of a bicycle. This camera setup and scene perspective is applicable to most kinds of electric vehicles. The lane boundaries are estimated with two straight lines on the left and right side of the lane and, where applicable, a third line at the far end of the visible road area. This approximation is close to the actual ego lane for many cases, but is limited to a straight lane course. In curves, the aim is the linearization of the ego lane at the current position with two straight lines using motion information.

The task entails following challenges: While the borders of streets are often clearly distinguishable from neighboring areas due to lane markings or clear material changes, the transitions can be smoother for pedestrian or bicycle areas, especially where vegetation is adjacent to the lane. Another difficult case occurs if shadows overlap the lane borders or if the lane borders are occluded through dirt or objects such as parking vehicles.

The contribution of this work is the development of a fast ego lane detection system that is suitable for personal light electric vehicle applications as it works in various road places. Using a combination of two line detection strategies and geometrically based rules, no large annotated data set is needed.

2 Related Work

Chougule et al. as well as Meyer et al. present deep learning approaches for lane border detection and lane segmentation in [1] and [2], respectively. Thereby, a mean IoU of 76.39% (cf. [1]) and 80.01% for ego lanes (cf. [2]) is yielded. However, their methods are not suitable for personal light electric vehicle applications with limited computation hardware. Furthermore, due to the dependency on datasets, results are significantly worse for pedestrian or bicycle lanes, as all training samples are taken from a car driver's perspective driving on a street.

Lane detectors based on traditional image processing methods are presented in [3] and [4]. For road area segmentation, in those works texture descriptors are used. We show that a simple distance function based on color information suffice, is faster to calculate and furthermore, better suited for the application on various lane types where the variance in road surface structures is high compared to solely street applications. In [4] and also in [5], the position of the vanishing point is used to enhance lane area prediction. As the geometrical conditions of scenes in driver's perspective give valuable information about the lane borders, we use this approach for selecting the corresponding lines from a set of candidates. We show that a fixed vanishing point estimation is sufficient for the approximation of straight lanes.

3 Methodology

The overall system goes through three phases for each image. First, lane border candidates are proposed using gradient and color image information. Secondly, the both candidates who best meet the geometric conditions of the scene are chosen as left and right border

line. Thirdly, based on the movement between the previous and the current image, it is decided whether the ego vehicle is currently driving a curve. If this is the case, with the aid of movement information, straight road lane boundaries are estimated, that linearize the curve at the current position.

Our approach specifically considers the following three traffic scenes:

1. The ego vehicle drives straight on a straight lane. The lane borders are rich in contrast. In this case, the lane borders can be extracted with traditional gradient-based edge detection methods. The approximation of the lane area with straight lines is suitable.
2. The ego vehicle drives straight on a straight lane, but the lane boundaries are not clear due to occlusions (e. g. vehicles parked on the roadside) or smooth transitions (e. g. vegetation at the roadside). In this case, the gradient based approach is unsuitable. Thus, the road surface is extracted using color-based segmentation. The approximation of the lane area with straight lines is suitable.
3. The ego vehicle drives along a curve. In this case, the two previous approaches may produce inappropriate results, because the condition of a straight roadway is not fulfilled. The goal in curves is the approximation of the actual roadway by linearization of the lane borders at the current position. For this purpose, the intersection point of the two linearized road edges is estimated using optical flow.

In the following, the three approaches introduced above are described in detail. Then, the final selection of the linearized roadway boundaries is presented. Finally, we quantitatively and qualitatively evaluate the results.

3.1 Gradient-based Lane Border Candidates

If the lane border is rich in contrast, e. g. due to road surface markings or a change in the pavement material, the lane borders can be

extracted with the Canny edge detector pursuant to [6]. To suppress high-frequency noise and high-frequency image structures, a bilateral filter is applied in a pre-processing step. Assuming that the lane borders are dominating lines in the image, they can be found in the gradient image with the Hough line transform according to [7]. The number of proposed lines depend on the scene. Typically, several lines are proposed with the gradient-based approach. See Figure 3.1 for an example.

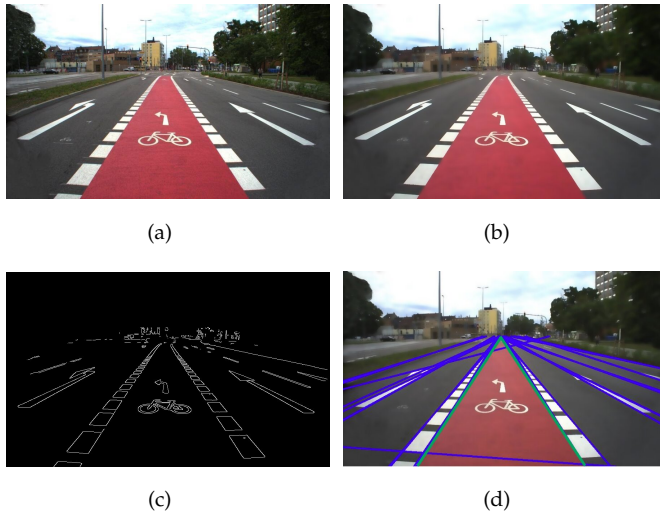


Figure 3.1: Visualization of the gradient-based lane border detection. (a) Input image. (b) Bilateral filtering applied. (c) Gradients found with Canny edge detector. (d) Lines found with Hough line transform, including the best candidates for lane border approximation in green.

3.2 Color-based Segmentation Lane Border Candidates

For each image, in addition to candidates based on gradients, color-based segmentation is used to extract the lane area and propose two further candidates using geometrical conditions of traffic scenes. This approach is aimed for situations where the road border line is not clear because of occlusions by plants or other objects. Despite

bilateral filtering, no lines are found at lane borders, if the transition is fluent on the one hand. On the other hand, edges extracted from vegetation does not allow to find the lane border line. Then, a high number of edges in different orientations are found near the actual lane border when the Canny edge detector is applied. For color-based segmentation of the lane area, a region of interest (ROI) is chosen in the lower center of the image. Assuming that most pixels of the ROI show the surface of the ego lane, a binary mask with pixels that may belong to the ego lane is created using a color-based distance function. The reference color is the average of all color values of the pixel in the ROI. Several options of distance functions for color images exist. For our application, best results are archived using a modified version of the CIE94 ΔE^* color distance definition as defined in [8]: For a reference color (L_1^*, C_1^*, H_1^*) and another color (L_2^*, C_2^*, H_2^*) defined in the CIELAB color space, the color distance is defined as

$$\Delta E_{94}^* = \sqrt{\frac{\Delta L^{*2}}{k_L S_L} + \frac{\Delta C^{*2}}{k_C S_C} + \frac{\Delta H^{*2}}{k_H S_H}}, \quad (3.1)$$

with ΔL^* being the lightness difference, ΔC^* being the chroma difference and ΔH^* being the hue difference. S_L , S_C and S_H are weighting functions that adjust the CIE differences $(\Delta L^*, \Delta C^*, \Delta H^*)$ according to the standard in CIE 1976 color space: $S_L = 1$; $S_C = 1 + 0.045C^*$; $S_H = 1 + 0.015C^*$. k_L , k_C and k_H are parametric weighting factors of the three components. To decrease the impact of lightning on the color distance, we choose a high value for k_L . In that way, shadows on the lane surface has less influence on the segmentation result.

By calculating the color distance for each pixel and thresholding, a binary image is created.

For proposing two lane borders in the binary image, the position of the vanishing point is used. We assume a fixed position of the vanishing point for a certain camera setup for simplicity and to show the robustness of our method. An important prerequisite is that the recorded images are in conformity with the perspective principle: Assuming that the left and right lane borders are straight, parallel and run in driving direction, they intersect in the vanishing point

in the image. Thus, assuming a straight and parallel lane, all possible lane border candidates identified from the binary road area image must run through the vanishing point. A second condition is, that the ratio of *lane pixel* to the number of all pixels on the line is higher than a certain threshold. For the color-based line detection, one line for each the left and right lane boundary is proposed that runs through the vanishing point, exceeds the *road pixel threshold* and has the maximum opening angle from all possible lines fulfilling the first and second condition.

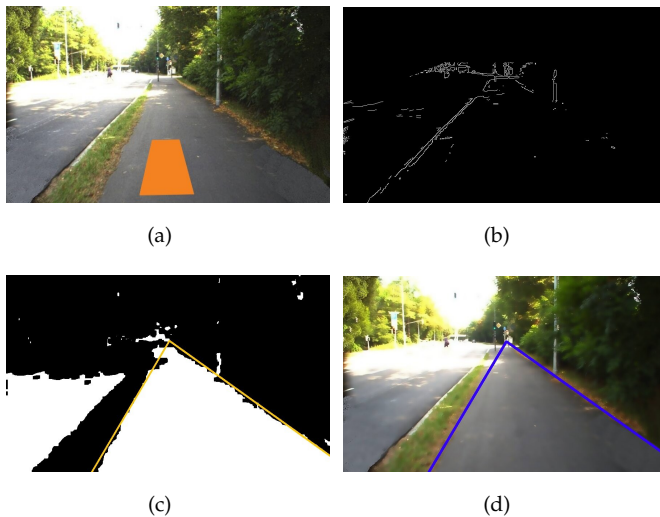


Figure 3.2: Visualization of the segmentation-based lane border detection. As shown in (b), the gradient-based approach fails in this case. (a) Input image with the ROI marked in orange. (b) Edges and lines found with Canny edge detector and Hough line transform. (c) Binary mask: white pixel: color distance to reference color below threshold (*lane pixel*), black pixel: above threshold. (d) Color-based candidates in input image.

3.3 Linearization of Curves using Motion Information

While the two methods above rely only on the current frame, the ego motion between the previous and current frame is used in the cases

of curves. More precisely, the sparse optical flow between the two frames is used to refine the intersection of the road edges, which was originally set as a fixed vanishing point. The idea is that the projection of the optical flow on the horizontal axis is a measure of how far the intersection point of the two border lines of the road must shift in the direction of the curve in order to achieve a linearization of the road at the current position. The linearization should approximate the actual lane course in the best possible way with straight lines and the IoU between the actual and the linear approximated lane surface should be optimized.

With the Lucas Kanade method, cf. [9], sparse optical flow vectors are calculated for feature points above the estimated horizon in both images. Then, noise, e. g. as a result of mismatched feature points is reduced with two-dimensional Density-Based Spatial Clustering of Applications with Noise (DBSCAN) for the vector length and direction. Details about the clustering method DBSCAN are given in [10]. For vectors of the dominating cluster, the average length in horizontal direction $|\bar{V}_u|$ is determined. To take into account the difference of the distance to the camera between the feature points and the vanishing point at the horizon, the displacement of the original point of intersection (poi), thus, the static vanishing point, is defined as $\Delta_{poi} = \pm |\bar{V}_u|^{1.25}$ with the sign selected according to the vector direction. Figure 3.3 visualizes the optical flow vector, the clustering and displacement of the point of intersection for a sample image.

In curves, the gradient- and color segmentation approach fails as the assumption of straight, parallel lane borders is not fulfilled. Instead, we use the assumption that the scene between two images differs only slightly and take the intersections of the roadway boundaries and the lower image border from the previous image. In that way, three image points are defined, which are the start and end point of the approximated lane boundaries.

3.4 Final Lane Border Selection

In 3.1 and 3.2 it is shown, how several lane border candidates are proposed. Following rules and conditions are applied to find the

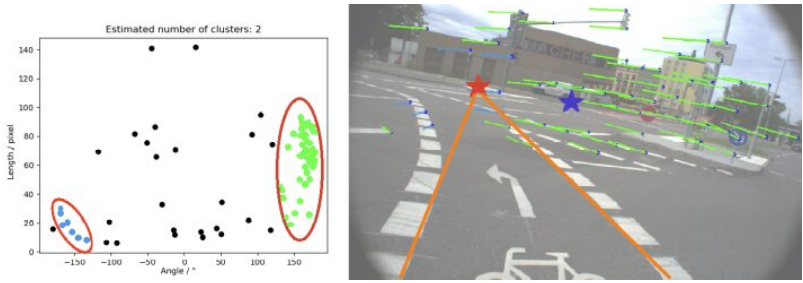


Figure 3.3: Visualization of poi refinement in curves. Left: Optical flow vectors in orientation - length space. The two dominating clusters found with DBSCAN marked with circles. Right: Optical flow vectors of two main clusters in input image. The blue star marks the position of the default vanishing point. The red star is the estimated point of intersection of the left and right lane border (orange lines).

two candidates that represent the left and right lane border most likely:

1. Assuming a straight road, the angle between the road border line and the horizontal image boundary is within a certain range. Experimentally determined are the ranges $[30^\circ, 80^\circ]$ and $[100^\circ, 150^\circ]$ for the left and right lane boundary, respectively.
2. Assuming straight, parallel lane boundaries, the both lines intersect in the vanishing point. Thus, the condition is set that the absolute horizontal distance of the point of intersection of the lane borders with the horizon to the position of the vanishing point should be below a certain threshold.
3. Of the remaining lines, the two whose intersection with the bottom edge of the image is farthest from the center are selected.

If the mean absolute length of the optical flow vectors $|\bar{V}_u|$ is above a certain threshold, it is assumed that the ego vehicle is driving on a curved lane. Then, two lane borders as described in 3.3 are taken as final selection.

3.5 Evaluation

We evaluated our approach on a total of over 1200 images from about 50 different traffic scenes sequences. The scenes include one- and multi-lane streets, bicycle lanes (separate, distinctly on streets, and besides pedestrian paths), and pedestrian paths, forest paths or parks. In most cases, the lane borders are predicted only with minor deviations from the actual position. Even though the true lane area can not be represented correctly in curves as the lane borders are limited to straight lines, the detected lane area overlaps widely for the majority of test samples. Most scenes for which errors occur, show wide, open roads and a high variations from the standard case of two parallel lane boundaries. For a quantitative analysis, we take the best possible linear approximation with two lines as ground truth. We reach a mean IoU between the area enclosed by the predicted and annotated lane borders and the button line of 75.71%. Figure 3.4 and 3.5 show representative results for straight lanes and curves.

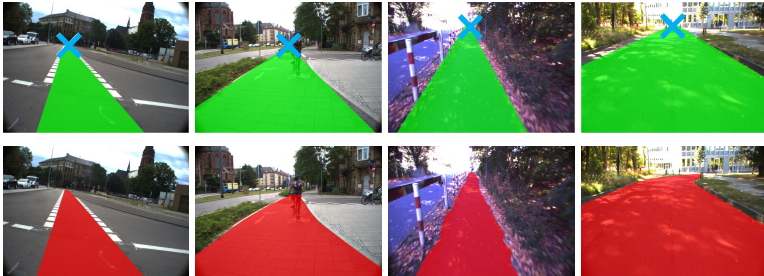


Figure 3.4: Representative results for straight streets, bicycle lanes and sidewalks. Top row: our results. The blue cross marks the point of intersection. Bottom row: ground truth.

4 Discussion and Summary

Although each step of the pipeline is fast and simple, the lane border detector is powerful and yields good results for various traffic types including streets, bicycle and pedestrian lanes comparable to deep

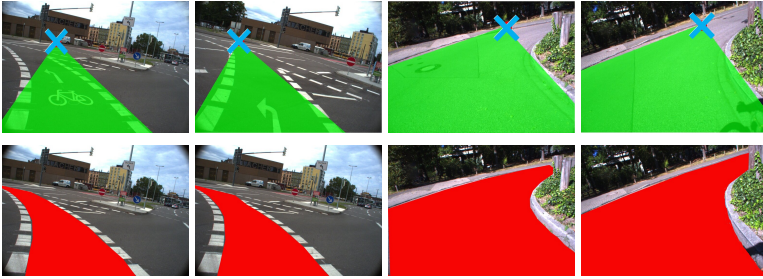


Figure 3.5: Representative results for curved streets, bicycle lanes and sidewalks. Top row: our results. The blue cross marks the point of intersection. Bottom row: ground truth.

learning approaches. Neither a large training data set or ground truth labels are needed, nor are parameters needed to be fine-tuned for the different lane types. Moreover, the algorithm can be to run on low-cost hardware in real-time, which make a great advantage over deep learning based approaches for applications on personal light electric vehicles.

References

1. S. V. Chougule, A. Ismail, G. Adam, V. Narayan, and M. Schulze, "Reliable multilane detection and classification using a compact encoder-decoder cnn," in *Forum Bildverarbeitung*, 2018, pp. 291–301.
2. A. Meyer, N. O. Salscheider, P. F. Orzechowski, and C. Stiller, "Deep semantic lane segmentation for mapless driving," in *2018 IEEE/RSJ International Conference on Intelligent Robots and Systems (IROS)*, 2018, pp. 869–875.
3. S. Graovac and A. Goma, "Detection of road image borders based on texture classification," *International Journal of Advanced Robotic Systems*, vol. 9, no. 6, p. 242, Jan. 2012. [Online]. Available: <https://doi.org/10.5772/54359>
4. H. Kong, J. Audibert, and J. Ponce, "General road detection from a single image," *IEEE Transactions on Image Processing*, vol. 19, no. 8, pp. 2211–2220, 2010.

R. C. Peter et al.

5. U. Ozgunalp and S. Kaymak, "Lane detection by estimating and using restricted search space in hough domain," *Procedia Computer Science*, vol. 120, pp. 148–155, 2017. [Online]. Available: <https://doi.org/10.1016/j.procs.2017.11.222>
6. B. Jähne, *Digitale Bildverarbeitung*. Springer Berlin Heidelberg, 2002. [Online]. Available: <https://doi.org/10.1007/978-3-662-06731-4>
7. J. Canny, "A computational approach to edge detection," *IEEE Transactions on Pattern Analysis and Machine Intelligence*, vol. PAMI-8, no. 6, pp. 679–698, 1986.
8. R. McDonald and K. J. Smith, "Cie94-a new colour-difference formula*," *Journal of The Society of Dyers and Colourists*, vol. 111, pp. 376–379, 2008.
9. B. Lucas and T. Kanade, "An iterative image registration technique with an application to stereo vision (ijcai)," vol. 81, 04 1981.
10. "A density based algorithm for discovering density varied clusters in large spatial databases," *International Journal of Computer Applications*, vol. 3, 06 2010.